Mask Defect Disposition: Flux-Area Measurement of Edge, Contact, and OPC Defects Correlates to Wafer and Enables Effective Decisions

Peter Fiekowsky [a1], Darren Taylor[b], David Wang [c], C.C. Yang [c], S.C. Lin [c] L.H Tu [d], K R Lin [d]

[a] Automated Visual Inspection, 952 S. Springer Rd. Los Altos, CA USA
[b] Photronics, 601 Millennium Dr. Allen TX, USA
[c] PSMC, Hsinchu, Taiwan
[d] UMC, Hsinchu, Taiwan

Presented at Photomask Japan 2001, Paper 4409-10, April 2001

ABSTRACT

Lithographers' ability to set useful defect and contact specifications has almost disappeared as chip geometries have shrunk. As features sizes have decreased, measurement error has increased to 25% of the maximum allowable defect size. Contact sizing has suffered similarly. This has made defect disposition so difficult that many processes now require that all detected defects be repaired because the automatic defect sizing is almost meaningless, that is, the required guard band is nearly the size of the defect specification (Reynolds, BACUS 2000).

Many mask processes have abandoned defect sizing in favor of stepper simulation, either using simulation microscope, such as AIMS, or software, such as NTI's VSS. However AVI's optical Flux-Area measurement technique provides accuracy and repeatability that gives the simple, time tested "defect specification" technique new life.

This study shows that high quality edge-, contact-, and OPC- defect disposition can be achieved using the Flux-Area technique. A test mask with a range of edge defects as well as mis-sized contacts and OPC defects was written. The defects on that mask were measured on an AVI Metrology System, and the mask was printed using a 0.15 µm process. The wafer defects were then measured on a SEM. The specifications are tested by printing a very different test pattern with the same process. The mask defect sizing performed with the AVI is shown to be consistent on different chips using the same process. Thus it is shown that all the over-spec defects on the wafer were measured as over-spec on the mask.

Results show that edge defect size on the wafer can be accurately predicted from the AVI defect area; that printed contact size is linearly proportional to the AVI measured area, on both square and irregular contacts; and that OPC defects (printed line-end separation errors) can be accurately predicted from AVI serif-area measurements on the mask.

With the Flux-Area measurement technique as implemented on the AVI Photomask Metrology System, defects can be measured with long term repeatability and rms repeatability between machines of better than 10 nm, 3% of a 0.3 µm defect. This means that guard bands can often be reduced from 0.15 µm to below 0.05 µm.

Keywords: Photomask Defect Disposition, Metrology, SEM, Flux-Area

INTRODUCTION

Shrinking chip feature geometries have forced similarly shrinking features on photomasks. As mask geometries approached the subwavelength (inspection wavelength) region in the mid-90s, maximum defect sizes declined well below the inspection wavelength. The result of this has been that accurate defect sizing has become nearly impossible using conventional edge-to-edge techniques. Meanwhile the viability of Aerial Imaging for defect evaluation on critical masks has become widely accepted.

This loss of ability to provide sensible defect measurements in many mask manufacturing processes has resulted in mask users demanding "zero defects" rather than zero defects above a threshold size. "Zero defects" is an expensive process because every defect repair reduces the mask quality, and has a high risk of inducing other harder-to-detect defects. Furthermore, "Zero defects" means "zero detectable defects", and the detectability of defects depends on the inspection

---

Correspondence for Peter Fiekowsky: Email: peter@aviphotomask.com; www.aviphotomask.com;
Phone +1-650-941-6871; Fax 650-941-4821;
Automated Visual Inspection, 952 S. Springer Road, Los Altos, CA 94024

tool and its setup. This has meant that disagreements between mask makers and wafer fabs have continued, if not increased.

The AVI Flux-Area measurement technique provides the repeatability and accuracy in defect sizing that is needed to allow sensible defect size specifications to be used again. The standard technique had been, and should continue to be that a wafer fab runs a test mask through its current process. The wafer is examined and the maximum acceptable defects sizes are for edge defects, isolated defects, contacts, and now line-ends (with or without OPC) are determined. The mask defects that generated those wafer defects are measured with the Flux-Area technique. Then the maximum defect size specifications are determined from the wafer and mask defect measurements, and given to the mask shop.

This study tested and validated the assertion that Flux-Area measurement provides sufficient accuracy to the wafer, and sufficient repeatability from tool to tool to allow defect specifications to be used effectively on leading edge masks. In addition, it demonstrated that mask contact shape has no effect on wafer contact size, that only mask contact area (Flux-Area) affects wafer contact size. It also demonstrated that the AVI flux-area technique is a reliable optical measurement of OPC line ends which correlates very closely to the wafer measure of line ends, line end shortening.

METROLOGY GOALS

In the macro world the goal of metrology is "Accurate measurements", where accuracy is usually traced back to NIST or similar standards. In the micro world of lithography the size of things depend on how you measure. An optical measurement will differ from electrical resistance size measurement, even if both are traceable to NIST standards.

Lithography process and wafer yield improvements require the following: 1) Accurate mask feature measurements; 2) Measurements repeatable from mask shop to fab. 3) Measurements that correlate to what prints, and are unaffected by the mask writing tool or process. 4) Fast, easy-to-calibrate measurements.

The word "accuracy" usually evokes "NIST" for most of us. Nevertheless the gold standard in lithography is not NIST's stamp, but simply feature size on the wafer. Thinking in the lithography field has shifted towards using the SEM as the gold standard for accuracy. This makes sense when measuring pattern fidelity in a mask writer. However defect and contact metrology are more related to wafer printability than pattern fidelity, so the gold standard is still the wafer when we are working to increase wafer yield and performance.

DEFECT METROLOGY METHODS

Conventional metrology techniques are linear, measuring the edge-to-edge size of features. Although sensible, this technique runs into several problems on modern photomasks. First of all, on features whose size approaches the wavelength of light being used to measure, the observed edge position of an edge depends highly on the position of nearby edges. This is why conventional metrology systems generally stop operating when the size to be measured gets to within 10% of the measuring wavelength.

Secondly, the linear size of a 2D feature, such as a defect, a contact, a line end, or a corner is not adequate to accurately describe the effect of that feature in the lithography process. Because the result on the wafer's photoresist depends on the total light flux at any position, the best measure of a lithographic feature's size is the amount of light flux that passes through it.

Even when using SEMs, edge-to-edge measurement has been a problem. One issue has been to determine what is the "real" edge. Edge profiles vary depending on etching techniques, so any one definition will not work well as etching varies. In addition, most 2D features are irregular at the size scale we are interested in, so sampling a few edge points is not sufficient. Some SEM software now samples all the edge points to solve this problem. SEM measurements have a number of other disadvantages related to the use of electrons rather than photons: Charging of isolated features, damage to the chrome, deposition of a thin film, and the requirement that any pellicle is removed, and it requires extra handling to be put into the SEM's vacuum chamber.

AVI's Flux-Area technique measures this light flux, generally bypassing the question of edge location that has confounded conventional measurements.

FLUX-AREA MEASUREMENT

The Flux-Area technique allows the measurement of features much smaller than λ, and provides accuracy and repeatability in the range of $\lambda/100$ (5 nm with visible light). Rather than edge to edge dimension, it measures optical area, which correlates to printability on the wafer.1 The technique consists of subtracting the background (Figure 1); integrating the total light flux that is transmitted by the feature (Figure 2), converting that flux to square pixels, and then scaling pixels to microns.

In the Flux-Area technique the clear-chrome contrast around the region of interest is measured, giving the chrome contrast in digitizer levels (milliwatts per pixel). Next a region of interest is defined which includes the feature to be measured plus enough margin to include 99% of the blurred light. The total flux from the feature (shaded area in Figure 2) is integrated, and divided by the chrome contrast,

$$\text{Flux-Area} = \sum_{x,y} (Ixy - Ibgrnd) / (Iclear - Ichrome)$$

where Ixy is the intensity of a pixel in the region of interest, Ibgrnd is the background intensity in the area of the feature, and the Flux-Area has units of square pixels. This area is converted into linear pixels either by taking the square root (assuming the feature is square), or by multiplying the area by $4/\pi$ before the square root, assuming the feature is round.

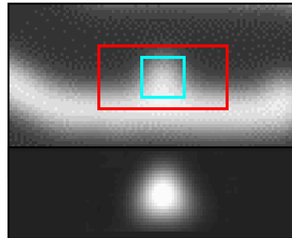

Figure 1. Subtracting the background to leave the feature flux only.

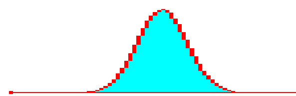

Figure 2. Integration of feature flux minus background.

The final step is scaling pixels to microns. This scale calibration is usually performed by measuring a line pitch on a known plate, and is normally repeatable to one part in 500. In Flux-Area measurement the largest error source is illumination uniformity, both spatial and temporal. Depending on the performance of the associated optics and electronics, and user procedures this limits repeatability to the range of one percent of the feature size.

The optical qualities of the imaging system (blurring) have very little effect on measurements. Moderate changes in focus have no effect because they don't affect the total light that detected by the camera. Similarly, other factors that affect optical resolution have very little effect.

STUDY DESCRIPTION

This study was performed with a binary COG mask designed by Photronics and PSMC, and written at PSMC on an Hitachi-800 e-beam writer, and dry-etched. The wafer was printed at UMC using a .15 µm process, with a Nikon S204 DUV 4X scanner, NA=.65, Sigma=.7, Exposure Energy/Focus = 30/-0.1. The wafer conditions were YS510_4.3K (Photoresist, ShinEtsu) & Bottom ARC(630A) on poly 1000K.

Two different test patterns on the mask were studied. The first was a simple edge defect test pattern consisting of four sets of parallel lines: two with widths of 0.6 µ and two with widths of 0.8 µ. Each line width had dense and isolated patterns, giving pitches of 1.0, 1.8, 5.6, and 5.8 µ. On these lines were placed clear intrusions ranging from 0.05 to 0.40 µ in 50 nm increments. This pattern was repeated on two chips to confirm repeatability across the mask and the wafer.

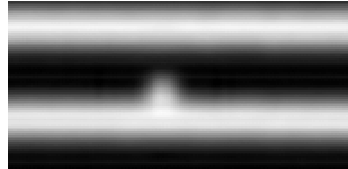

Figure 3. Sample edge defect in the edge defect pattern.

The second pattern, Figure 4, called "C" pattern, was an OPC Pattern with 0.5 µm lines, 0.32µm assist lines, typical pitch of 0.7 µm, and four sets of defects, each ranging in size from -0.25 µm to +0.25 µm. The defect types were: edge extensions/intrusions (to confirm the edge defect printability from the simple pattern), line-end OPC serif defects, mis-sized contacts, and contacts with corner defects.

Figure 4. Sample of "C" pattern, edge defect.

The mask was measured using the AVI Flux-Area technique using images acquired from a KLA363 using 0.25 µm pixels, and from a KMS 400, using white light and g-line, with a100x 0.95 NA objective. Both were calibrated using the 5.8 µm pitch on the test pattern.

The wafer was measured on a KLA 8100 SEM at UMC. The corner defect contacts were too irregular to measure with the standard SEM software, so those contact areas were measured with the AVI algorithms, tuned for SEM images.

EDGE DEFECTS

Figure 5 shows the correlation between the wafer measurements and the Flux-Area measurements, taken from the KLA images. Note that the mask measurements are plotted as area (not diameter), and that the mask defect area is generally linearly related to the wafer defect width. The reason for this relationship is that the light on the wafer is blurred by approximately the wavelength of the stepper, 248 nm. Thus an edge defect on the wafer will always be smeared into a long (248 nm) bulge, as seen in Figure 6. The area of the defect on the wafer is linearly proportional to the area of the mask defect; however, the width of the defect has the same relationship because the length of the defect is essentially constant for the small defects we are concerned with.

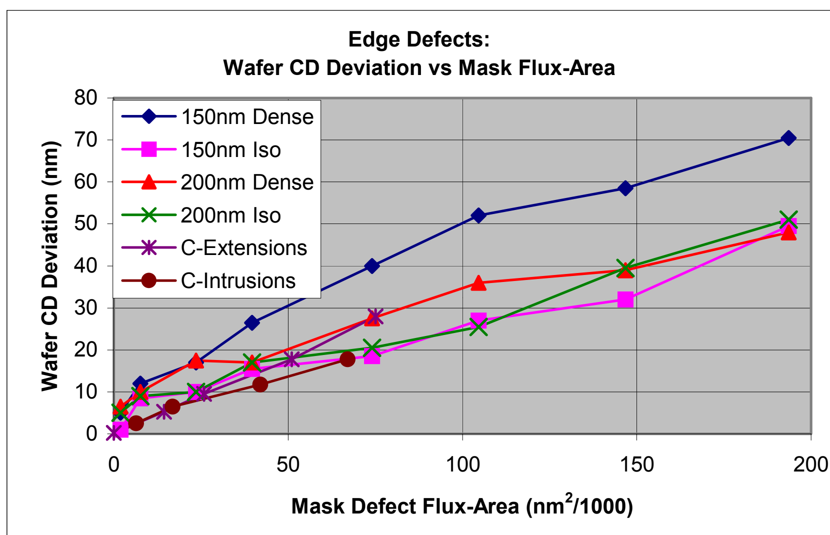

Figure 5. Edge defect correlation: Mask to wafer. Note linear correlation between mask defect area and wafer CD Deviation. Five defect types have the same slope; the 150 nm Dense (wafer pitch=.25µ) has 30% higher slope

Figure 5 shows the printability of edge defects in six different situations. The first set, the defects on 150 nm dense lines, stands out as different from the other sets. This pattern is much denser than the others, with a pitch of 1 µ; the next most-dense pattern is the "C-pattern", the OPC pattern, with a pitch o 1.7 µ. The other patterns range from 1.8 µto 5.8 µ pitch. One can see that defects on pattern pitches 1.7 µ or more have the same printability in this process, where the CD error on the wafer is equal to the mask defect area divided by 4 (for the scanner ratio) and divided by 248, for the mean length of the defect. The defects on the 1 µ pitch pattern printed 30% larger than that (MEEF=1.3)., presumably because of proximity effects.

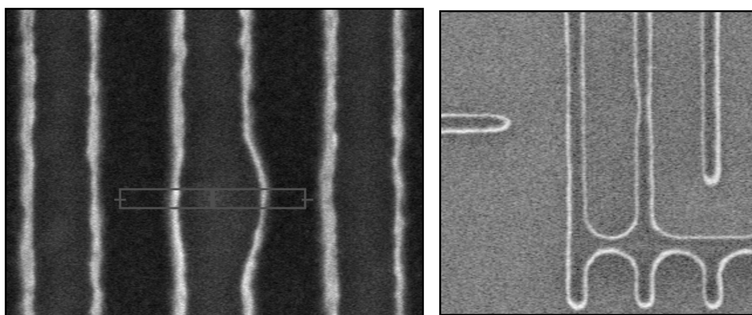

Figure 6. 71 nm clear intrusion on a 150 nm dense (pitch = 1µ) line, and 28 nm. clear intrusion on the OPC pattern (pitch = 1.7µ).

CONTACTS

Figure 7 shows the correlation between the wafer measurements and the Flux-Area measurements, taken from the KLA images. As expected, there is a simple linear relationship between the mask contact area and the wafer contact area.

Note that the printability of the contacts was the same for the symmetrical mis-sized contacts and for the irregular “corner defect” contacts. Thus measuring mask contact shape does not help predict the wafer contact size. The mask contact’s effective area (Flux-Area) is the only mask parameter required to predict the wafer contact size. Figure 8 shows representative contacts on the mask and on the wafer.

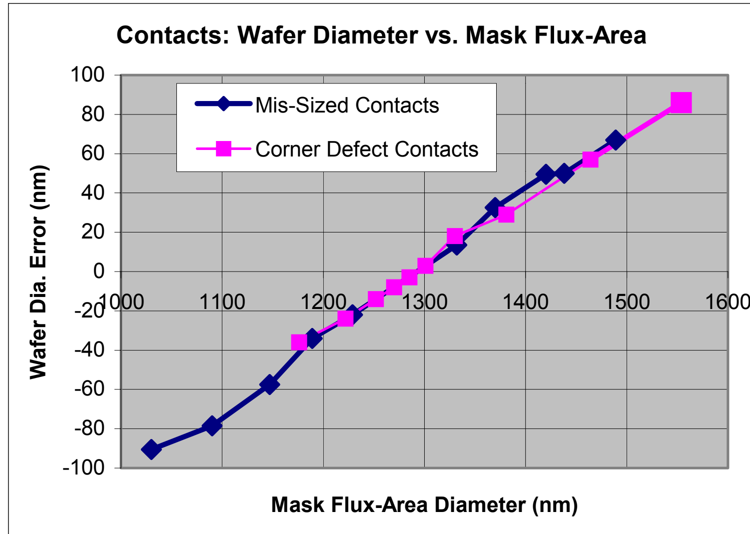

Figure 7. Contact defect correlation: Mask to wafer. Note that the correlation between mask area and wafer is the same for both square and irregular shaped contacts.

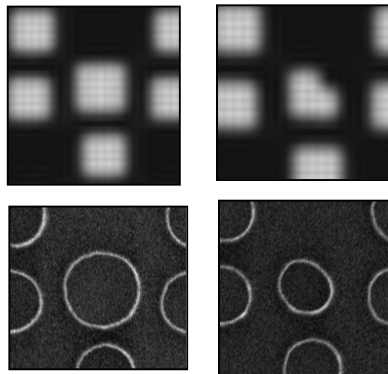

Figure 8. Mis-sized and corner-defect contacts. Mask (top) and wafer.

OPC LINE ENDS

Figure 9 shows the linear correlation between the AVI mask serif area and the wafer line-end separation. There is an inverse linear relationship between the square root of the Mask serif area and the wafer line end separation. The mask serif area is measured by subtracting the normal line from the serif line end, and summing the extra flux from the serif area. The AVI also provides mask line-end separation measurements which can indicate incorrect line separation even when the serif area is correct. Figure 10 shows samples of the mask and wafer line-end images. After a linear fit to the data the AVI serif area predicted the wafer line-end separation with a sigma of 1.9 nm and a range of 5 nm.

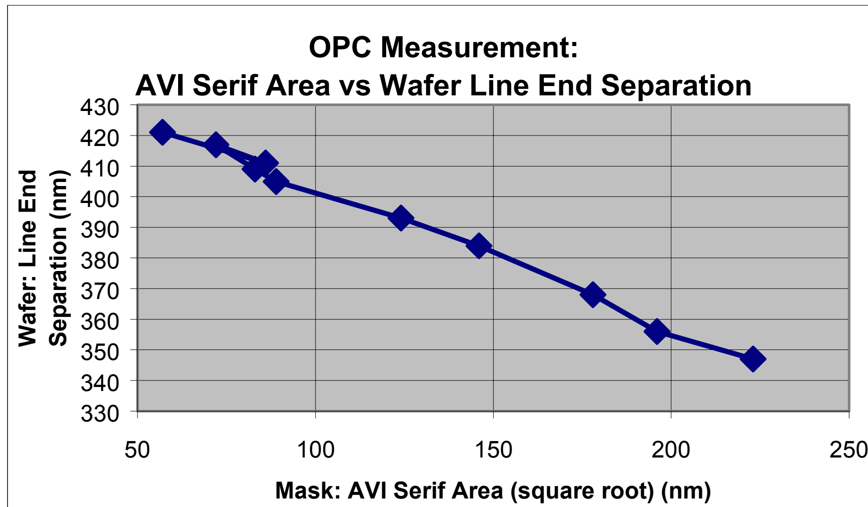

Figure 9. OPC defect correlation: Note linear correlation between AVI Mask OPC area and wafer line-end separation.

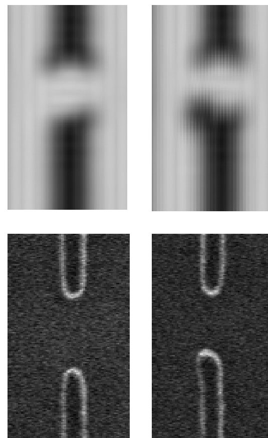

Figure 10. Sample OPC Serif defects. Mask (top) and wafer. Left side is an undersized serif, right side is over-sized.

CROSS-PLATFORM CORRELATION:

Figure 11 shows the difference between measurements of edge defects using KLA 365nm images, and the same defects imaged with KMS using g-line and white light. This shows that the same defects can be measured on very different platforms, and give the same result within 25 nm. The noise level on the “C” pattern data is higher than the noise on the edge defect pattern because one set of data was taken on the KMS in white light and the other in G-line. The G-line images were lower intensity, and thereby noisier. The image noise mostly affects small defects, where the noise sometimes has more contrast than the defect. In the future this can be avoided by averaging images, as is now done with the KLA images.

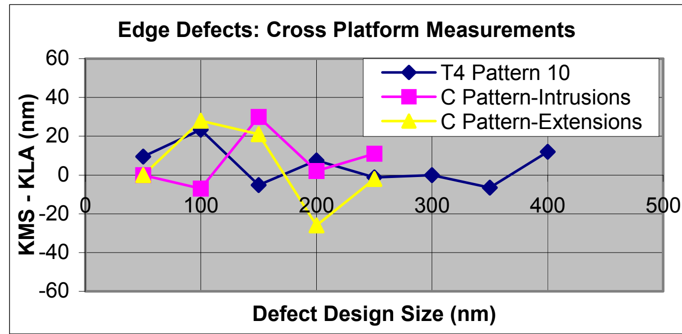

Figure 11. Difference between Flux-Area measurements of the same edge defects using KMS-400 white light images, minus measurements using KLA363 I-line images.

CONCLUSIONS

This study has shown very good correlation between measured sizes of mask defects, using AVI's Flux-Area technique, and their resulting wafer defects. This suggests that this new defect metrology makes real defect disposition based on test masks viable at least down to the 150 nm process node. Further, the data suggests that the flux area technique can be extended, by image averaging, to smaller nodes.

Flux-Area measurements usefully predicts wafer edge defect sizes. The data show that defect printability is constant over a wide range of patterns, down to a pitch of approximately half the scanner wavelength. For less dense patterns (MEEF=1) the printed edge defect size is equal to the mask defect area divided by the scanner magnification squared (the area magnification), divided by the scanner wavelength. When the wafer line pitch was reduced to the scanner wavelength the printed defects were 1.3 times larger than predicted (MEEF = 1.3), linear over a size range up to 72 nm (58% linewidth deviation).

The data shows that contact printability depends on mask contact area, and is independent of the contact shape (over a moderate range). Thus the simple measure of total flux through a contact is an excellent measure of the contact size. Traditional measurements of defect size on a contact are thus only useful as secondary predictors of contact area errors.

Flux-Area OPC measurements are shown for the first time to be highly correlated to wafer line-end separation. This means that the printability of mask OPC defects can be determined with two simple parameters, the OPC (flux) area, and the OPC (flux) separation. A value of either one outside the desired range will produce a wafer line-end separation defect, and values of both within range predict strongly no wafer defect. AVI to wafer deviation was 2nm at 1σ

The data indicate that the Flux-Area technique can give the same results at mask shop & wafer fab. Because calibration is very simple, correct calibration is easily assured. This should allow better communication of specs between fabs and mask shops.

Finally, the Flux-Area technique is shown to usefully measure defects as small as 100 nm with visible light or I-line illumination.

FUTURE WORK

This study covered a number of areas, each of which calls for significant further work. In edge defect measurement, improved noise immunity for edge defects smaller than 100nm is needed. In addition, similar testing for isolated defects, especially determining at what distance from an edge an isolated defect starts acting like an edge defect. This can be calculated theoretically, but that theory needs to be tested.

Some new areas that need to be examined include: repair damage measurement—how well does Flux-Area measurement (especially at other than the scanner wavelength) predict wafer errors? Also, similar studies with attenuated and alternating phase shift masks need to be done.

Finally, the integration of defect metrology into defect inspection is begging to be accomplished.

REFERENCES

1. P. Fiekowsky, Defect printability measurement on the KLA-351: Correlation to defect sizing using the AVI Metrology System, 19th Annual BACUS Symposium on Photomask Technology and Management, 1999.